

# CHEMISTRY

## A European Journal

A Journal of



### Accepted Article

**Title:** Towards Monodisperse Star-Shaped Ladder-Type Conjugated Systems: Design, Synthesis, Stabilized Blue Electroluminescence and Amplified Spontaneous Emission

**Authors:** Wen-Yong Lai, Yi Jiang, Mei Fang, Si-Ju Chang, Jin-Jin Huang, Shuang-Quan Chu, Shan-Ming Hu, Cheng-Fang Liu, and Wei Huang

This manuscript has been accepted after peer review and appears as an Accepted Article online prior to editing, proofing, and formal publication of the final Version of Record (VoR). This work is currently citable by using the Digital Object Identifier (DOI) given below. The VoR will be published online in Early View as soon as possible and may be different to this Accepted Article as a result of editing. Readers should obtain the VoR from the journal website shown below when it is published to ensure accuracy of information. The authors are responsible for the content of this Accepted Article.

**To be cited as:** *Chem. Eur. J.* 10.1002/chem.201605885

**Link to VoR:** <http://dx.doi.org/10.1002/chem.201605885>

Supported by  
**ACES**

WILEY-VCH

# Towards Monodisperse Star-Shaped Ladder-Type Conjugated Systems: Design, Synthesis, Stabilized Blue Electroluminescence and Amplified Spontaneous Emission

Yi Jiang,<sup>[a]</sup> Mei Fang,<sup>[a]</sup> Si-Ju Chang,<sup>[a]</sup> Jin-Jin Huang,<sup>[a]</sup> Shuang-Quan Chu,<sup>[a]</sup> Shan-Ming Hu,<sup>[a]</sup> Cheng-Fang Liu,<sup>[a]</sup> Wen-Yong Lai,<sup>\*[a,b]</sup> Wei Huang<sup>[a,b]</sup>

**Abstract:** A novel series of monodisperse star-shaped ladder-type oligo(*p*-phenylene)s, named as TrL-*n* (*n* = 1-3), have been explored. Their thermal and electrochemical properties, fluorescence transients, photoluminescence quantum yields, density functional theory calculations, electroluminescence (EL) and amplified spontaneous emission (ASE) properties have been systematically investigated to unravel the molecular design on optoelectronic properties. The resulting materials showed excellent structural perfection free of chemical defects, exhibiting great thermal stability ( $T_d$ : 404-418°C and  $T_g$ : 147-184°C) and amorphous glassy morphologies. Compared with their corresponding linear counterparts FL-*m* (*m* = 1-3), TrL-*n* showed only little bathochromic shifts (5-12 nm) for the absorption maxima  $\lambda_{max}$  in both solution and films. The star-shaped ladder-type compounds exhibited enhanced optical stability and suppressed low-energy emission. Their EL spectra exhibited excellent stability with increasing the driving voltage from 6 to 12 V. Moreover, superior low ASE thresholds were recorded for TrL-*n* compared with FL-*m*. Rather low ASE threshold (29 nJ/pulse or 1.60  $\mu$ J/cm<sup>2</sup>) was recorded for TrL-3, demonstrating their promising potential as excellent gain media. This study provides a novel design concept to develop monodisperse star-shaped ladder-type materials with excellent structural perfection, which are vital for shedding light on exploring robust organic emitters for optoelectronic applications.

## Introduction

Nowadays,  $\pi$ -conjugated organic semiconductors have been widely explored with the rapid advancement of organic electronics.<sup>[1]</sup> Among them, star-shaped molecules constitute an important class of organic electronic materials,<sup>[2]</sup> which usually comprise a central core and multiple conjugated arms as the functionalized units. By means of combining the merits of small molecules and polymers, star-shaped molecules have received

considerable interest in the field of organic optoelectronics, which possess huge advantages of well-defined structures, excellent flexibility, great thermal stability, good film-forming characteristics, and superior optoelectronic properties.<sup>[3]</sup> Previous studies have shown that various cores such as truxene,<sup>[4]</sup> isotruxene,<sup>[5]</sup> benzene,<sup>[6]</sup> pyrene,<sup>[3a,7]</sup> triazatruxene,<sup>[8]</sup> triphenylamine,<sup>[9]</sup> triazine,<sup>[10]</sup> and spirofluorene<sup>[11]</sup> have been employed to construct various star-shaped molecules. Consequently, it is particularly gratifying that recent progress in organic synthesis provides the possibility of designing and synthesizing novel materials with complex branches and bulky structures to achieve promising functional characteristics like polymers with high molecular weights.

Phenylene-based conjugated oligomers and polymers are promising candidates for organic electronics due to their high photoluminescence quantum efficiency, prominent charge-carrier mobility, and great electrochemical and thermal stability. Since the first report on ladder-type poly(*p*-phenylene)s (LPPP) by Scherf and Müllen in 1991,<sup>[12]</sup> various ladder-type materials based on phenylene building blocks have been synthesized and investigated in the field of organic optoelectronics.<sup>[13]</sup> Due to their efficient blue emission, ladder-typed  $\pi$ -conjugated polymers are promising conjugated materials for optoelectronic applications, such as organic light-emitting diodes (OLEDs), and organic lasers.<sup>[14]</sup> However, in the solid state, the emission of ladder-type polymers is unstable due to the appearance of long-wavelength emission bands, which has been attributed to physical or chemical degradation processes.<sup>[13b, 15]</sup> Apart from these, in the process of polymer analogous reactions, fully bridged polymers are subjected to incomplete formation of bridges. A tiny quantity of ketonic defects in the polymers, which even can't be detectable by means of UV-visible and infrared (IR) spectroscopy measurements, can lead to a drastic change of the emission spectra in the solid state especially under driving voltages. This is mainly because the ketonic defects in films are low-energy trapping sites, which are generally accompanied by efficient energy transfer. Therefore, it is highly desirable to develop ladder-type conjugated materials with excellent structural perfection free of ketonic defects to achieve superior spectral stability. Intense efforts have been attempted to address this challenge. For instances, by modifying the synthesis of LPPP previously reported by Scherf and Müllen,<sup>[12]</sup> Ma's group replaced benzene-diboric acid with 9,9-dihexylfluorene-2,7-bis(boronic acid pinacol ester) to accomplish a novel series of ladder-type conjugated polymers with improved structural perfection.<sup>[13a]</sup> Bo et al. developed a new synthetic approach to develop spiro-bridged ladder-type polymers and oligomers with excellent thermal and color stability.<sup>[13c]</sup> Nevertheless, the attempt on constructing star-shaped ladder-type conjugated

[a] Y. Jiang, M. Fang, S.-J. Chang, J.-J. Huang, S.-Q. Chu, S.-M. Hu, Dr. C.-F. Liu, Prof. Dr. W.-Y. Lai, Prof. Dr. W. Huang  
Key Laboratory for Organic Electronics and Information Displays, Institute of Advanced Materials (IAM), Jiangsu National Synergetic Innovation Center for Advanced Materials (SICAM)  
Nanjing University of Posts & Telecommunications  
9 Wenyuan Road, Nanjing 210023, China  
E-mail: iamwylai@njupt.edu.cn

[b] Prof. Dr. W.-Y. Lai, Prof. Dr. W. Huang  
Key Laboratory of Flexible Electronics (KLOFE) & Institute of Advanced Materials (IAM), Jiangsu National Synergetic Innovation Center for Advanced Materials (SICAM)  
Nanjing Tech University (NanjingTech)  
30 South Puzhu Road, Nanjing 211816, China

Supporting information for this article is given via a link at the end of the document.

systems with excellent structural perfection free of chemical defects is rare.<sup>[13k, 16]</sup>

In this contribution, we present a design strategy to explore a novel series of monodisperse star-shaped ladder-type oligo(*p*-phenylene)s, named as TrL-*n* (*n* = 1-3), with the aim to achieve excellent structural perfection free of chemical defects. The novel star-shaped systems are composed of truxene as the central core, three fused ladder-type oligo(*p*-phenylene) arms with varying  $\pi$ -conjugated length and diphenylamine units as functional end-cappers. Ladder-type oligo(*p*-phenylene) arms were fused into the star-shaped conjugated system in order to take the significant advantages of rigid conjugated ladder-type architectures to improve the carrier mobility and thermal and electrical stability of monodisperse star-shaped systems. Truxene comprising three overlapping fluorene units was selected as the central core to construct fully-fused conjugated star-shaped ladder-type system with phenylene building blocks. Diphenylamine units were used as the end-cappers, which are expected to modulate the electronic energy levels and thus the charge injection/transport properties.<sup>[6, 13e, 17]</sup> In the interest of unraveling how the molecular design affects the optoelectronic properties, corresponding linear counterparts named as FL-*m* (*m* = 1-3), which contained the same  $\pi$ -conjugated system in every arm of TrL-*n*, were synthesized. The thermal, photophysical, electrochemical, electroluminescence (EL) and amplified spontaneous emission (ASE) properties of the resulting star-shaped ladder-type macromolecules were systematically investigated in comparison with those of their linear counterparts. Significantly, no obvious low energy green emission was observed from the resulting large star-shaped ladder-type conjugated systems for the TrL-*n* films annealed even at 200 °C for 30 min. Their EL spectra exhibited excellent stability with increasing the driving voltage from 6 to 12 V. Moreover, superior low ASE thresholds were recorded for TrL-*n* compared with their corresponding linear ladder-type counterparts FL-*m*.

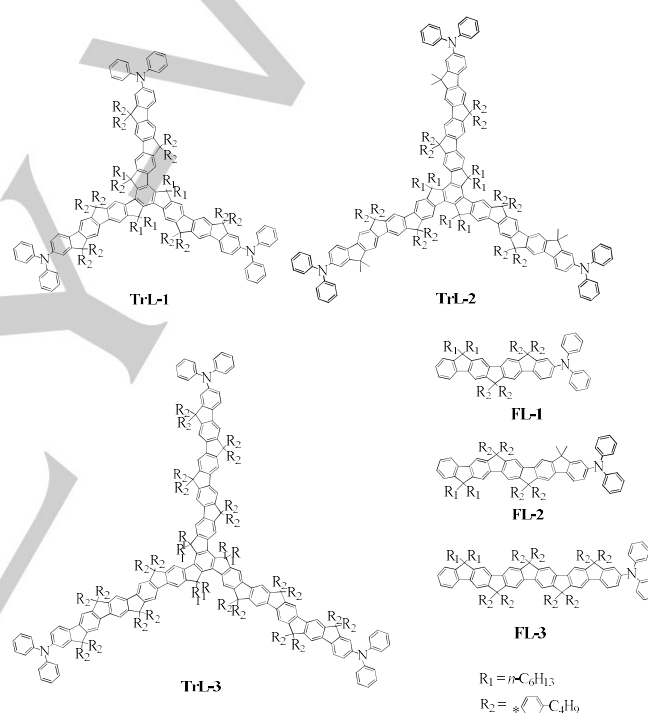
## Results and Discussion

### Synthesis and Structure Characterization

The chemical structures of TrL-*n* (*n* = 1-3) and FL-*m* (*m* = 1-3) are depicted in Scheme 1. Although truxene derivatives mainly based on three-substituted core scaffold have been widely studied,<sup>[4, 17b, 18]</sup> the star-shaped ladder-type systems based on truxene core remain largely unexplored.<sup>[13k, 16]</sup> Due to the facile functionalization at C-2, C-7, and C-12 positions and C-5, C-10, C-15 positions of truxene units, star-shaped ladder-type oligo(*p*-phenylene)s were constructed successfully by stepwise synthetic strategy.

The synthetic route to the ladder-type conjugated arms is outlined in Scheme 2. To prepare the diphenylamine end-capped ladder-type arms, it is necessary to synthesize the key monomer 4. Starting from the known reagent 1, 4-dibromo-2,5-benzenedicarboxylic acid, monomer 4 was obtained *via* a two-step synthesis in a total yield of 72%. The intermediate 1 was

obtained by palladium-catalyzed Suzuki cross coupling of excess monomer 4 with *N,N*-diphenyl-4-(4,4,5,5-tetramethyl-1,3,2-dioxaborolan-2-yl)aniline in a yield of 65%. The stepwise preparation of the key intermediate 2 commenced with the synthesis of 5, which was subjected to the amination of the aryl bromide by a modified, mild Buchwald cross-coupling reaction. Subsequent borylation using bis(pinacolato)diboron afforded the desired boronic acid pinacol ester 6. By using Suzuki cross-coupling reactions of building block 4 with 6, the intermediate 2 was obtained. Reaction of excess 4 with 1,4-benzenedi-boronic acid pinacol ester afforded 7 in a higher yield of 63% *via* microwave-accelerated Suzuki reactions.<sup>[4b]</sup> Palladium catalyzed Suzuki coupling of *N,N*-diphenyl-4-(4,4,5,5-tetramethyl-1,3,2-dioxaborolan-2-yl)aniline and monomer 7 afforded ladder-type arm 3 in 70% yield.

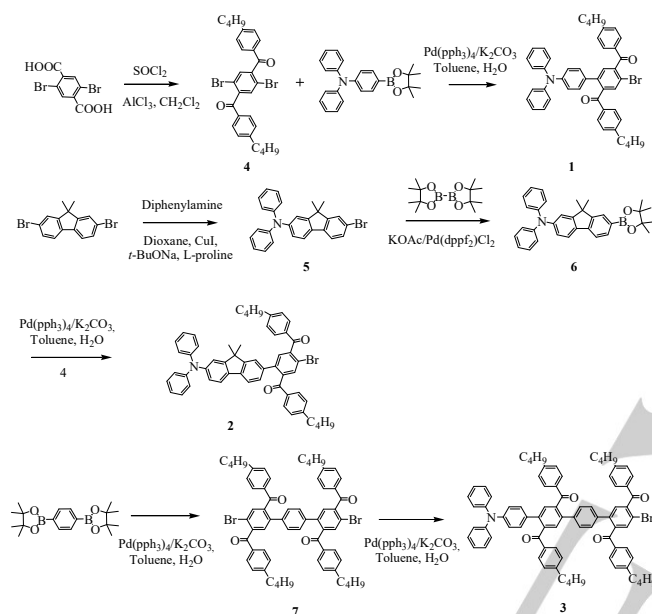


**Scheme 1.** Molecular structures of TrL-*n* and FL-*m*.

The synthesis of TrL-*n* adopted a convergent synthetic strategy by linking a truxene core and three corresponding arms. The synthetic strategy and detailed procedures for TrL-*n* are illustrated in Scheme 3. The monomer 8 was prepared *via* the route published by Pei et al.<sup>[19]</sup> Suzuki-Miyaura cross coupling of the boronic acid functionalized truxene core 8 and the bromo functionalized ladder-type arms formed the phenyl ketone-containing phenylene precursor Tr-1, Tr-2, Tr-3, respectively. The subsequent nucleophilic carbonyl addition and intramolecular Friedel-Crafts alkylation reactions afforded the fully ring-bridged ladder scaffolds of TrL-*n*.

The synthesis of FL-*m* was similar to the preparation of TrL-*n*, as shown in scheme S1. The well-defined structures and

chemical purities of the intermediates and the final ladder-type macromolecular stars and linear counterparts have been adequately verified by  $^1\text{H}$  NMR,  $^{13}\text{C}$  NMR, MALDI-TOF mass spectrometry. The  $^1\text{H}$  and  $^{13}\text{C}$  NMR spectra of the phenyl ketone-containing phenylene precursors (Tr-1, Tr-2, Tr-3, F-1, F-2, F-3) and final targets (TrL-n, FL-m) were given in Figure S1-S24. The eluting curves from the gel permeation chromatography (GPC) (Figure 1 and Table S1) exhibited symmetrical narrow peaks with polydispersities of  $\leq 1.01$ , suggesting a very high monodispersity and purity. No distinct precursors or partially substituted byproducts were observed.



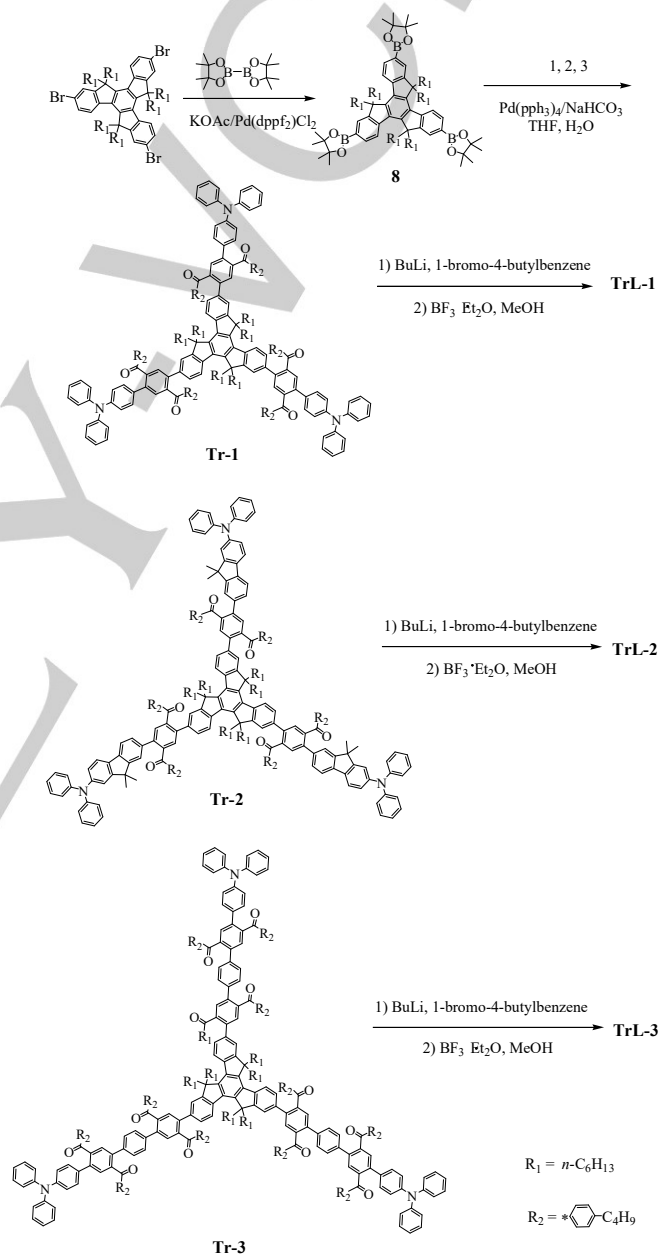
**Scheme 2.** Synthetic routes towards the ladder-type arms (Compounds 1-3).

### Thermal stability

The thermal stabilities of the resulting ladder-type star-shaped macromolecules TrL-n and linear counterparts FL-m were investigated by thermogravimetric analysis (TGA) and differential scanning calorimetry (DSC) in an inert  $\text{N}_2$  atmosphere, as shown in Figure 2 and Table 1. For the star-shaped ladder-type macromolecules TrL-n, good thermal stability of the compounds was confirmed by TGA with high decomposition temperatures ( $T_d$ , corresponding to 5% weight loss) in the range of 404–418 °C. The reason for the weight lost to around 50% of the original weight might be the cleavage of alkyl or aryl substitution at the bridgeheads in ladder-type oligophenylenes.

According to DSC curves, TrL-n exhibited their glass transition temperatures ( $T_g$ ) between 147–184 °C, which increased with increasing the  $\pi$ -conjugated phenylene rings. Moreover, compared with the linear counterparts FL-m,  $T_g$  of the ladder-type macromolecules rised obviously by ca. 70 °C. The  $T_g$  values of TrL-n are also generally higher than those of the three-

armed<sup>[4a,20]</sup> and even six-armed<sup>[4b,6,21]</sup> oligofluorene counterparts. The results suggested the high rigidity of the fused star-shaped ladder-type conjugated systems. As revealed by DSC curves, both TrL-n and FL-m exhibited glassy morphologies with no obvious melting processes during the repeated scan cycles. According to wide-angle X-ray diffraction (WAXD) patterns (Figure S25), no obvious diffraction peak was observed, further confirming their amorphous glassy morphologies.



**Scheme 3.** The synthesis towards the ladder-type macromolecular stars TrL-n.

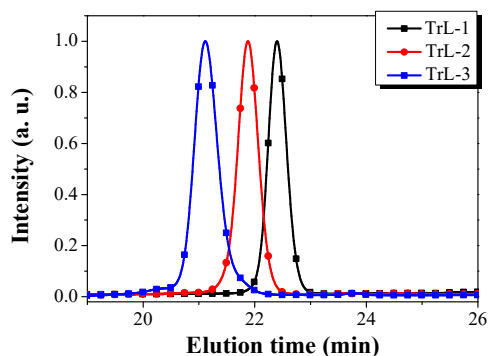


Figure 1. The GPC elution curves of TrL-n.

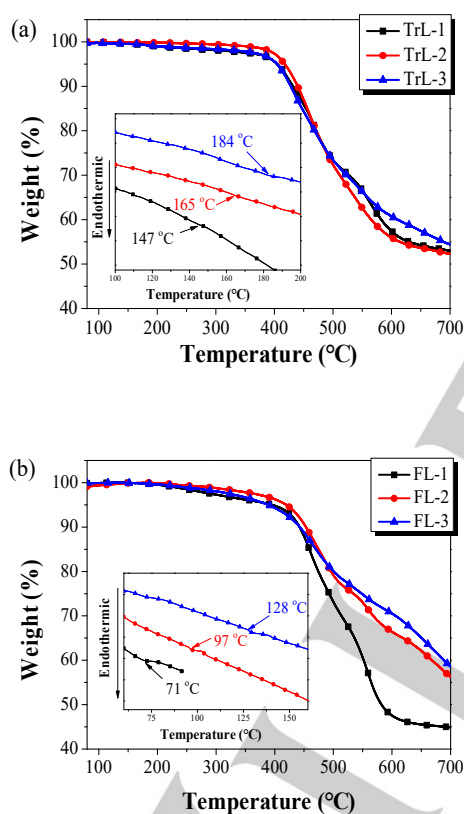


Figure 2. TGA and DSC curves of the materials recorded at a heating rate of  $10\text{ }^{\circ}\text{C min}^{-1}$ .

### Optical properties

Optical properties of TrL-n were investigated in comparison with those of their corresponding linear counterparts (FL-m). The absorption and emission spectra of the samples measured in

dilute THF ( $1\times 10^{-6}\text{ M}$ ) and neat films are shown in Figure 3 and Figure 4, respectively. The results are summarized in Table 1. According to our previous report, different flexible side chain plays an important role on modulating the functional properties of organic semiconductors for optoelectronics.<sup>[22]</sup> We here mainly focus on the effect of the phenylene rings number on the photochemical and electrochemical properties. The impact of molecular design will be elucidated by comparing TrL-n with the linear ladder-type counterparts FL-m.

In dilute solution, the UV/Vis absorption spectra of all compounds are mainly composed of two bands: the  $n\rightarrow\pi^*$  transition of triarylamine moieties and the  $\pi\rightarrow\pi^*$  transition of the ladder-type skeleton. For TrL-n, the UV/Vis absorption spectra have presented a well-defined vibronic structure with two main absorption peaks at 388 nm and 410 nm for TrL-1, 395 nm and 419 nm for TrL-2, 405 nm and 430 nm for TrL-3, respectively. Obviously, the absorption spectra undergo bathochromic shifts (9-11 nm) with increasing the number of phenylene rings. In comparison with the corresponding linear ladder counterparts FL-m, the absorption spectra of TrL-n show obvious bathochromic shifts (7-10 nm), indicating the existence of additional  $\pi$  delocalization between the rigid ladder-type skeleton arms through the truxene core.

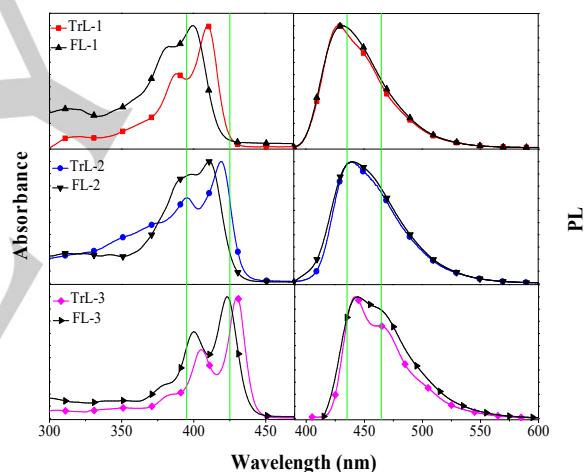


Figure 3. Normalized absorption and fluorescence spectra for TrL-n ( $n = 1-3$ ) and FL-m ( $m = 1-3$ ) in  $10^{-6}\text{ M}$  THF at room temperature. The four vertical lines denote the positions of 395, 425, 435 and 465 nm for the view of the results of absorption and fluorescence spectra.

Unlike most linear rigid  $\pi$ -system such as LPPP and MeLPPP,<sup>[13a,13c]</sup> the absorption and fluorescence spectra of TrL-n ( $n = 1-3$ ) and FL-m ( $m = 1-3$ ) show poor mirror symmetry, which is also obviously different from other linear and star-shaped  $\pi$ -conjugated systems based on oligofluorenes.<sup>[4b]</sup> Furthermore, TrL-n show large Stokes shifts (12-18 nm), quite different from those rigid ladder-type counterparts without diphenylamine end-cappers that exhibit only very small Stokes shifts.<sup>[13a-c, 13g, 23]</sup> But the fluorescence spectra of TrL-n are quite similar to those of the corresponding linear FL-m, suggesting

**Table 1.** Photophysical Properties of the TrL-n and FL-m.

Compd	$T_d^{[a]}$ [°C]	$T_g^{[b]}$ [°C]	$\lambda_{max,abs}$		$\lambda_{max,PL}$		HOMO <sup>[e]</sup> / LUMO <sup>[f]</sup> [eV]	$\eta_{sol.}^{[g]}$	$\eta_{film}^{[g]}$	Estimated fluorescence lifetimes	
			[nm]		[nm]					$\tau_{THF}$ [ns]	$\tau_{film}$ [ns]
			THF <sup>[c]</sup>	Film <sup>[d]</sup>	THF <sup>[c]</sup>	Film <sup>[d]</sup>					
TrL-1	405	147	388, 410	392, 416	428	427, 451	-5.39/-2.55	0.81	0.30	1.29	0.28(68%), 2.98(32%)
TrL-2	418	167	395, 419	401, 425	437	436, 463	-5.37/-2.57	0.80	0.27	1.11	0.26(69%), 2.73(31%)
TrL-3	404	184	405, 430	409, 435	442, 467	451, 473	-5.34/-2.61	0.89	0.32	0.93	0.26(63%), 2.96(37%)
FL-1	396	71	381, 400	387, 408	432	427, 446	-5.37/-2.47	0.89	0.22	1.50	0.28(72%), 2.93(28%)
FL-2	420	97	391, 411	399, 420	440	434, 457	-5.37/-2.55	0.78	0.26	1.42	0.24(61%), 3.18(39%)
FL-3	392	128	400, 423	405, 423	445	448, 468	-5.33/-2.63	0.82	0.24	1.14	0.25(70%), 3.26(30%)

<sup>[a]</sup>  $T_d$ : decomposition temperature. <sup>[b]</sup>  $T_g$ : glass transition temperature. <sup>[c]</sup> Measured in  $10^{-6}$  M THF solution. <sup>[d]</sup> Film samples. <sup>[e]</sup> Estimated from the onset oxidation : reduction potential by using  $E_{HOMO} = -[E_{ox}+4.77]$  eV,  $E_{(Fe/Fe^+)} = 0.03$  eV. <sup>[f]</sup> Deduced from HOMO and  $E_g$  estimated from the red edge of the longest absorbpt wavelength for the solid-state films. <sup>[g]</sup> Fluorescence quantum yields in solution and solid-state films, measured on the quartz plate using an integrating sphere.

similar emissive decays for both the star-shaped and linear ladder-type conjugated systems.

The UV/vis spectra of TrL-n and FL-m in thin films are almost identical to their corresponding solution spectra, except for 3-7 nm bathochromic shifts. The fluorescence spectra of TrL-n in neat films show two well resolved emission bands, which can be assigned to the 0-0 and 0-1 singlet transitions. In addition, the emission spectra of TrL-n in neat films are practically identical to those obtained from corresponding FL-m, except for little slight red shifts of 2-6 nm. The results suggest that the bulky star-shaped architectures can effectively maintain the photophysical properties of the linear ladder-type skeletons even in the aggregation states.

The photoluminescence quantum yields (PLQYs) for TrL-n and FL-m in  $10^{-5}$  M THF and neat films are summarized in Table 1. All of the materials exhibited similar PLQYs in solution ( $\eta = 0.78$ -0.89), which are larger than the solid-state PLQYs, which are in the range from 0.22 to 0.32. The rapid decrease (over 2.5-fold) of  $\eta$  in the neat film suggested strong concentration quenching due to the large coplanar  $\pi$ -conjugated system. Among these materials, TrL-n show relatively higher PLQYs in the solid states, mainly due to the bulky star-shaped architectures that hinder the intermolecular interactions.

To study the excited state relaxation dynamics in the star-shaped ladder-type macromolecules, fluorescence transients of TrL-n and FL-m were investigated in  $10^{-5}$  M THF solution and in neat films (Figure 5). The corresponding data of fluorescence lifetime ( $\tau$ ) for TrL-n and FL-m are summarized in Table 1. The transients at the spectral peak of 0-1 band in neat films of all samples are shown in Figure S26.

Excited state relaxation of the samples in dilute solution was found to follow a quite similar single exponential decay profile with estimated fluorescence lifetimes ( $\tau$ ) of 1.14-1.50 ns for FL-m and a little shorter ones (0.93-1.29 ns) for TrL-n. The values of  $\tau$  showed a progressive decrease with the increase of the  $\pi$ -conjugated phenylene rings in the star-shaped system, which was similar to the trend of the linear counterparts. Star-shaped

ladder-type macromolecules showed relatively shorter lifetimes compared with the linear counterparts, suggesting more efficient intramolecular energy transfer and faster decays for the star-shaped ladder-type conjugated systems.

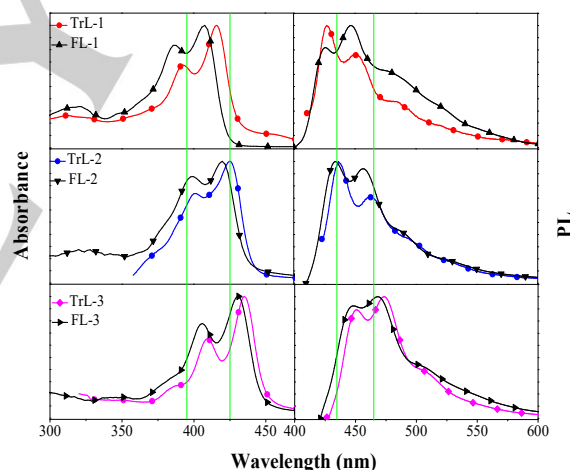


**Figure 4.** Normalized absorption and fluorescence spectra for TrL-n ( $n = 1$ -3) and FL-m ( $m = 1$ -3) in neat films at room temperature. The four vertical blue lines denote the positions of 395, 425, 435 and 465 nm for the discussion of the results of time-resolved fluorescence anisotropy.

Preliminary studies showed that fluorescence transients of thin films manifested bi-exponential behaviors, which included comparatively faster excited relaxation during the first 2 ns upon excitation and a slower relaxation state at a later stage. The bi-exponential transient together with the redshifted fluorescence emission in thin films suggested that energy transfer occurred. The fluorescence decay profiles were well described by two-component exponential decay models to clarify different components and their corresponding intensities, as summarized

in Table 1. The fractional intensity of different components is listed in the brackets adjacent to the  $\tau$  value, denoting various contributions to the whole excited-state decay. Obviously, the major contribution provided by the short component with  $\tau < 1.0$  ns, which was about one third of that recorded from the dilute solution, was probably ascribed to the fast radiative relaxation arising from the efficient exciton decays in thin films at the initial stage. The longer decay component mainly resulted from the stronger exciton delocalization or exciton migration, which was able to evade the fast radiative decays. According to the results, no significant differences in transient decays were noticed between the star-shaped ladder-type macromolecules and the corresponding linear counterparts, indicating that the molecular architecture has little impact on the fluorescence transients in film states.

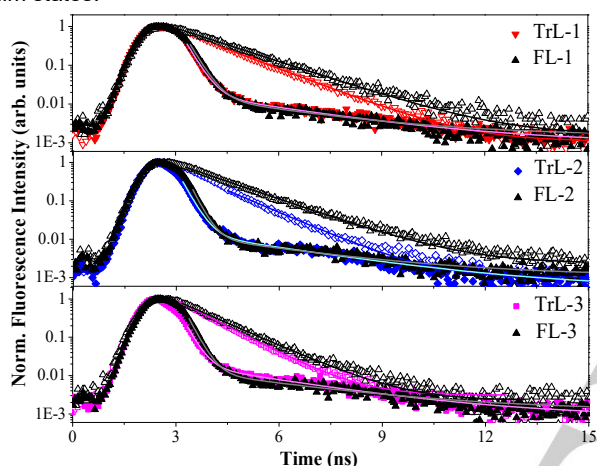


**Figure 5.** Fluorescence transients of  $10^{-5}$  THF solutions (open points) and neat films (solid points) of (a) TrL-1 and FL-1, (b) TrL-2 and FL-2, (c) TrL-3 and FL-3 excited at the first peak of fluorescence spectra. All of the lines indicate single or double exponential fits to the experimental data. Fluorescence lifetimes ( $\tau$ ) are indicated.

### Electrochemical Properties

The electrochemical behaviors of the compounds were investigated by cyclic voltammetry (CV) with a standard three-electrode electrochemical cell in acetonitrile solution containing 0.1 M tetrabutylammonium hexafluorophosphate (TBAPF<sub>6</sub>) at room temperature (Figure 6 and Figure S27). The oxidation potentials were measured versus Ag/AgNO<sub>3</sub> as the reference electrode and a standard ferrocene/ferrocenium redox system as the internal standard for estimating the highest occupied molecular orbital (HOMO) energy levels of the star-shaped ladder-type macromolecules and the linear counterparts. Figure 6 shows the CV curves of TrL-n in films at a scan rate of 20 mV/s in the range of 0–1.4 V. All the films exhibit irreversible oxidation process. The oxidation onset potentials are around 0.6 V, which can be attributed to the oxidation of the terminal diphenylamine groups. The corresponding HOMO energy levels are thus estimated to be around  $-5.37 (\pm 0.03)$  eV for TrL-n,

which are estimated from the onset reduction potentials assuming the absolute energy level of Fc/Fc<sup>+</sup> to be 4.8 eV below vacuum.<sup>[24]</sup> The band gaps ( $E_g$ ) of TrL-n, on the basis of the absorption onset of the solid-film samples, are estimated to be 2.84 eV, 2.80 eV, 2.73 eV for TrL-1, TrL-2 and TrL-3, respectively. By increasing the linear length of the ladder systems, the band gap becomes narrower (Table S2). The lowest unoccupied molecular orbital (LUMO) levels are thus calculated according to the following equation:  $E_{\text{LUMO}} = E_{\text{HOMO}} + E_{\text{gap}}$ . The results are summarized in Table 1 and Table S2.

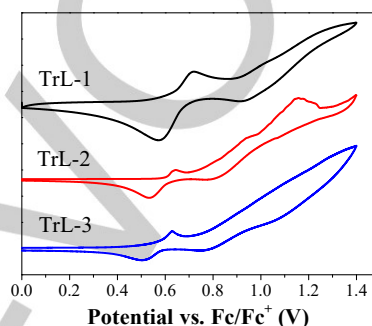


**Figure 6.** Cyclic voltammograms of TrL-n in CH<sub>2</sub>Cl<sub>2</sub> for oxidation.

### Theoretical Calculations

To gain insight into the electronic structure of TrL-n, density functional theory (DFT) calculations were carried out for the ground-state ( $S_0$ ) geometry optimization. To expedite the calculations, all the solubilizers on the saturated carbons are replaced with methyl groups. Singlet transition energies and spatial distributions of electron density for HOMOs (0, -1, -2) and LUMOs (0, +1, +2) are obtained by means of the semi-empirical ZINDO calculations. The energy diagram of the HOMO, LUMO and the nearby orbitals (HOMO-2, HOMO-1, LUMO+1, LUMO+2) for TrL-n and FL-m are shown in Figure 7. The frontier molecular orbitals (MOs) for TrL-1 are shown in Figure 8, and the corresponding frontier MOs for other molecules are shown in Figure S28-S32.

As shown in Figure 7, phenylene rings and molecular dimensions affect the orbital energy levels. It should be noted that the  $S_n \leftarrow S_0$  ( $n = 1, 2, 3$ ) excitation is primarily described by the energy transition from HOMOs (HOMO-2, HOMO-1, HOMO) to LUMOs (LUMO, LUMO+1, LUMO+2), although increasing the conjugated  $\pi$ -system can facilitate configuration interactions.<sup>[1d, 13k, 25]</sup> What's more, the little energy difference between HOMO-2 and HOMO-1 orbitals and LUMO+1 and LUMO+2 orbitals for TrL-n (Figure 7) can significantly increase the participation of the configurations associated with the HOMO-2 and LUMO+2 orbitals in the allowed transitions. The close HOMOs as well as LUMOs in the configuration of TrL-n is beneficial for the intramolecular charge transfer.

Although TrL-n have different phenylene rings, great similarity is observed in the electron distribution (Figure 8 and Figure S28-

29). In the case of TrL-1 (Figure 8), all the HOMOs are mainly localized on the selected end-capped diphenylamine moieties and adjacent ladder-type skeletons, which matches well with diphenylamine moieties as the strong electron donor. In contrast, all the LUMOs have electron density localized on the partially phenylene backbone including the central truxene core. Evidently, electron density distribution of every arm is not the same in all frontier MOs, which indicate that the  $\pi$  delocalization and excitation migration between the rigid ladder-type skeleton arms are suppressed. It is consistent with the similar absorption and fluorescence spectra for TrL-1 and FL-1. In this context, the same phenomena are also observed in the frontier MOs of TrL-2 and TrL-3 (Figure S28-29) and the electron distribution of FL-n (Figure S30-32).

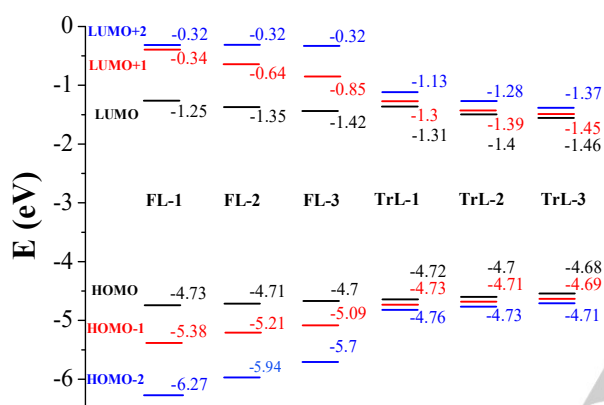


Figure 7. B3LYP/6-31G\*\* orbital energy level diagrams for TrL-n and FL-m.

### Optical Stability and Blue Electroluminescence

To determine their overall stability against the unwanted low-energy emission band at 2.2-2.4 eV, spin-coated films of all samples on quartz substrates were exposed to oxygen under thermal stress conditions in an accelerated lifetime test. The film samples were annealed at various temperatures (100 °C, 120 °C, 150 °C, 180 °C and 200 °C) for 30 min in open ambient atmosphere with room temperature of 25 °C and humidity of 30%. Figure S33-36 show UV/Vis spectra and fluorescence spectra of as-prepared films and the subsequently annealed ones in air at different temperatures. For the linear counterparts, upon thermal annealing at 180 °C or 200 °C (180 °C for FL-1, 200 °C for FL-2 and FL-3), the fluorescence spectra show broad bands between 500 and 600 nm. By comparison, Figure 9 shows the emission spectra of as-prepared films and the subsequently annealed ones at 150 °C and 200 °C in air for the star-shaped ladder-type macromolecules. From room temperature to 150 °C, all of the films exhibit no notable spectral shifts. Further increasing the temperature up to 200 °C, for TrL-1, the 0-2 emission band (2.4-2.7 eV) exhibits an obvious increase, and the low energy band at 2.2-2.4 eV increases with ongoing degradation. Upon increasing the temperature, TrL-2 exhibits

much better spectral stability without obvious energy increase in 0-2 emission band. But the energy increase is still recorded in the low energy band. In addition, TrL-3 shows no sign of an ongoing formation of low-energy emission at 200 °C. According to the analysis, the star-shaped ladder-type configuration can result in not only increasing spectral stability but also decreasing the low-energy emission, which holds great promise as blue emitters. The intensity change of 0-0, 0-1 and 0-2 emission peaks upon heating is mainly related to the structural relaxation energy and the associated vibrational mode.<sup>[26]</sup> It is thus inferred that the alkyl substitution at the truxene core and the bridgeheads in ladder-type oligophenylenes could reduce the stability towards oxidative degradation.<sup>[13b]</sup>

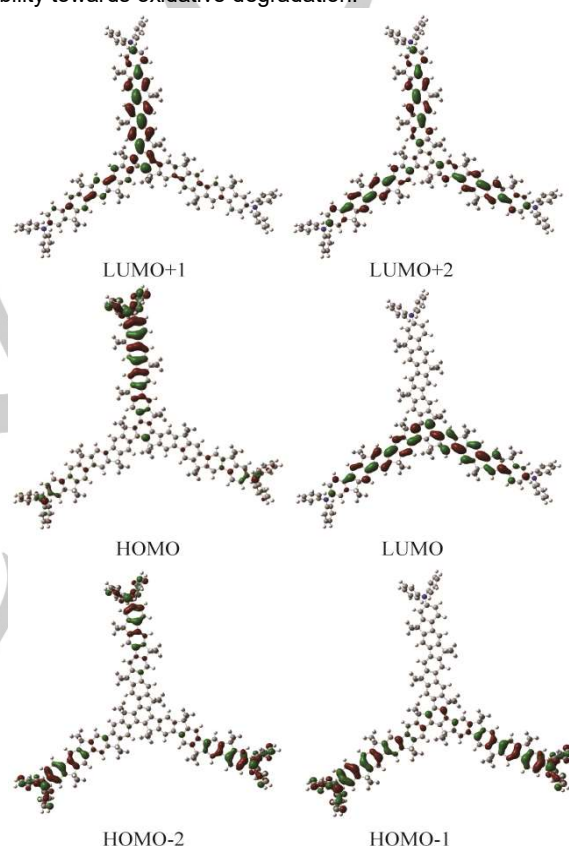
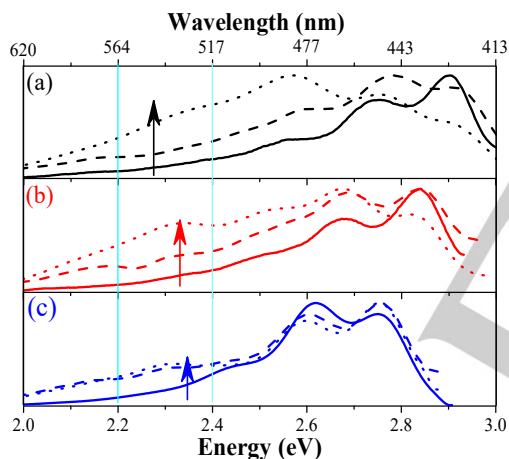


Figure 8. B3LYP/6-31G\*\* orbital energy level diagrams for TrL-n and FL-m.

To further investigate the luminescence properties of these star-shaped ladder-type macromolecules and the corresponding linear counterparts, especially their color stability under electrical bias, solution-processed OLEDs with the configuration of indium tin oxide (ITO)/PEDOT:PSS (40 nm)/emissive layer (EML, 50 nm)/1,3,5-tris(*N*-phenylbenzimidazol-2-yl)-benzene (TPBI, 30 nm)/lithium fluoride (LiF, 1 nm)/aluminum (Al, 100 nm) (emitter: TrL-n, (n = 1-3) Device A-C, respectively; FL-n, (n = 1-3) Device D-F, respectively) were fabricated, where TPBI was used as a buffer electron-transporting and hole-blocking layer.

The recorded EL spectra of TrL-1 (Device A, Figure 10a) are appreciably broader than the corresponding PL spectra (Figure 4), with a central peak at 452 nm, shoulder peaks at 432 nm and 480 nm. With increasing the  $\pi$ -system, the EL spectra (Device B and C, Figure 10b and c) show narrower emission and relatively more stable spectra across the range of driving voltages from 6 to 12 V. Compared with their PL spectra in the thin film states, the 0-0 emission bands are suppressed in the EL spectra, indicating more efficient energy transfer during the EL process. Notably, with increasing the driving voltage from 6 to 12 V, the EL spectra of the resulting devices based on TrL-n remain nearly unchanged, and the CIE coordinate values show negligible variation (Table S3), suggesting a remarkable voltage-independent EL emission. While the low-energy emission becomes more pronounced for the devices based on the linear counterparts (Device D-F) with an obvious change of the EL spectra observed as the devices were driven to higher luminance (Figure S38). The EL results presented here suggests that the bulky star-shaped ladder-type architectures with suppressed molecular alignment in the solid state are less prone to low-energy emission during the device operation. Additional EL characteristics of the devices are also supplied as summarized in Table S3.



**Figure 9.** The normalized PL spectra of (a) TrL-1, (b) TrL-2, (c) TrL-3 before and after annealing in air. The solid line: room temperature; dash line: 30 min at 150 °C; dot line: 30 min at 200 °C. Room temperature is 25 °C and the humidity is 30%.

### Amplified Spontaneous Emission (ASE) Properties

Organic emitters with good thermal and spectral stabilities are promising gain media for organic solid-state lasers. To explore this potential, ASE characteristics of TrL-n and FL-m have been investigated. In order to quantify our results, the pulse energy of exciting light at which the full width at half-maximum (FWHM) intensity of the emission spectra drops to half of its PL value was defined as the ASE threshold ( $E_{th}$ ).<sup>[27]</sup>

As shown in Figure 11 and Figure S39, the ASE peaks occur at 0-1 vibronic, corresponding to a favorable four-level gain

process, and eventually grow to dominate the spectra, namely at 457 nm for TrL-1, 465 nm for TrL-2, 477 nm for TrL-3, 450 nm for FL-1, 460 nm for FL-2, 473 nm for FL-3. ASE threshold ( $E_{th}$ ) values are 76 nJ/pulse (4.22  $\mu\text{J}/\text{cm}^2$ ) for TrL-1, 74 nJ/pulse (4.12  $\mu\text{J}/\text{cm}^2$ ) for TrL-2, 29 nJ/pulse (1.60  $\mu\text{J}/\text{cm}^2$ ) for TrL-3, 132 nJ/pulse (7.36  $\mu\text{J}/\text{cm}^2$ ) for FL-1, 161 nJ/pulse (8.40  $\mu\text{J}/\text{cm}^2$ ) for FL-2, 80 nJ/pulse (4.43  $\mu\text{J}/\text{cm}^2$ ) for FL-3, respectively (Figure S40 and S41, and Table 2). All the ASE results of TrL-n and FL-m are summarized in Table 2. Compared with the linear counterparts, the star-shaped ladder-type macromolecules exhibit much lower ASE thresholds, suggesting that the star-shaped ladder-type macromolecules are potential excellent gain media. Emphatically, the largest star-shaped ladder-type conjugated system TrL-3 achieves the lowest ASE threshold of 29 nJ/pulse (1.60  $\mu\text{J}/\text{cm}^2$ ), which is also among the best results reported for organic gain media.<sup>[3b, 22, 28]</sup>

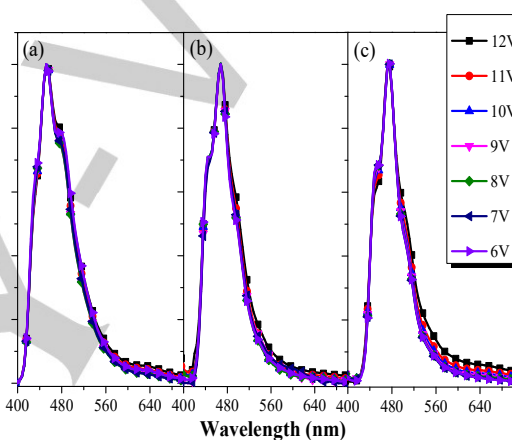


**Figure 10.** Normalized EL spectra of Devices (a) A (b) B (c) C at various driving voltages.

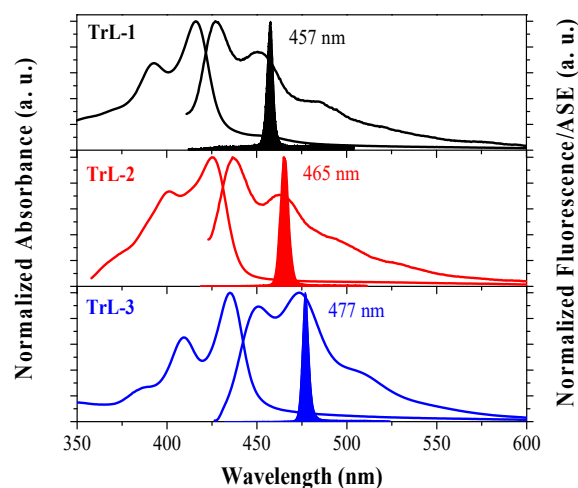


**Figure 11.** Normalized absorption, emission and ASE spectra (excited at 390 nm for TrL-1 and TrL-2 and excited at 405 nm for TrL-3) of the films of star-shaped ladder-type macromolecules.

**Table 1.** ASE properties of TrL-n and FL-m.

Compd	$\lambda_{\text{max, PL}}$ (nm)	$\lambda_{\text{ASE}}$ (nm)	FWHM (nm)	ASE threshold		
				energy/ pulse (nJ/pulse)	areal energy density ( $\mu\text{J}/\text{cm}^2$ )	areal power density ( $\text{KW}/\text{cm}^2$ )
TrL-1	427, 451	457	4.0	76	4.22	0.84
TrL-2	436, 463	465	4.2	74	4.12	0.82
TrL-3	451, 473	477	4.1	29	1.60	0.32
FL-1	427, 446	450	4.3	132	7.36	1.47
FL-2	434, 457	460	4.1	151	8.40	1.68
FL-3	448, 468	473	4.4	80	4.43	0.89

## Conclusions

We have successfully designed and synthesized a novel series of star-shaped ladder-type conjugated systems with excellent structural perfection accompanying well-defined structures, high chemical purity and no ketonic defects, named as TrL-n ( $n = 1-3$ ), based on oligo(*p*-phenylene)s with truxene core and diphenylamine end-cappers. The novel star-shaped ladder-type molecular design endows the materials with a robust bulky multi-dimensional molecular geometry that helps to define  $\pi$  delocalization. The resulting molecules exhibited not only good optical stability (especially for TrL-3) but also suppressed low-energy emission. It is worthwhile to mention that the EL spectra maintained nearly unchanged with increasing the driving voltages for the resulting star-shaped ladder-type macromolecules as the emitters. The results confirm that the bulky star-shaped ladder-type architectures with suppressed molecular stacking in the solid states are less prone to low-energy emission during the device operation. Star-shaped ladder-type macromolecules are also found to exhibit much lower ASE thresholds, manifesting their great potential act as excellent gain media for organic lasers. This study provides a novel design concept to develop monodisperse star-shaped ladder-type materials with excellent structural perfection, which are vital for shedding light on exploring robust organic emitters for optoelectronic applications.

## Acknowledgements

The authors acknowledge financial support from the National Key Basic Research Program of China (973 Program, 2014CB648300), the National Natural Science Foundation of

China (21422402, 21674050, 20904024, 61136003), the Natural Science Foundation of Jiangsu Province (BK20140060, BK20130037, BM2012010), Program for Jiangsu Specially-Appointed Professors (RK030STP15001), Program for New Century Excellent Talents in University (NCET-13-0872), Specialized Research Fund for the Doctoral Program of Higher Education (20133223110008), the Ministry of Education of China (IRT1148), the NUPT "1311 Project" and Scientific Foundation (NY213119, NY213169), the Synergetic Innovation Center for Organic Electronics and Information Displays, the Priority Academic Program Development of Jiangsu Higher Education Institutions (PAPD), the 333 Project (BRA2015374) and the Qing Lan Project of Jiangsu Province.

**Keywords:** conjugated systems • star-shaped ladder-type molecules • oligo(*p*-phenylene)s • electroluminescence • amplified spontaneous emission

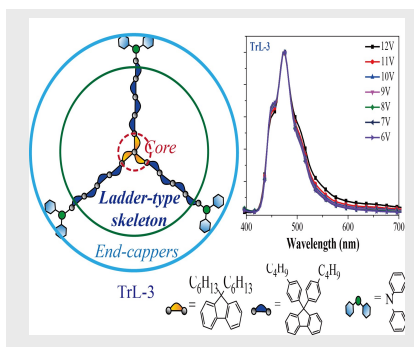
- [1] a) Y. Liu, J. Zhao, Z. Li, C. Mu, W. Mu, H. Hu, K. Jiang, H. Lin, H. Ade, H. Yan, *Nat. Commun.* **2014**, *5*, 5293; b) Q. Zhang, B. Kan, F. Liu, G. Liu, X. Wan, X. Chen, Y. Zuo, W. Ni, H. Zhang, M. Li, Z. Li, F. Huang, Y. Huang, Z. Liang, M. Zhang, T. P. Russell, Y. Chen, *Nat. Photonics* **2015**, *9*, 35-41; c) S. Hirata, Y. Sakai, K. Masui, H. Tanaka S. Y. Lee, H. Nomura, N. Nakamura, M. Yasumatsu, H. Nakanotani, Q. Zhang, K. Shizu, H. Miyazaki, C. Adachi, *Nat. Mater.* **2015**, *14*, 330-336; d) L.-H. Xie, C.-R. Yin, W.-Y. Lai, Q.-L. Fan, W. Huang, *Prog. Polym. Sci.* **2012**, *37*, 1192-1264.
- [2] a) A. L. Kanibolotsky, I. F. Perepichka, P. J. Skabara, *Chem. Soc. Rev.* **2010**, *39*, 2695-2728; b) S.-C. Lo, P. L. Burn, *Chem. Rev.* **2007**, *107*, 1097-1116.
- [3] a) T. Qin, W. Wiedemair, S. Nau, R. Trattning, S. Sax, S. Winkler, A. Vollmer, N.Koch, M. Baumgarten, E. J. W. List, K. Müllen, *J. Am. Chem. Soc.* **2011**, *133*, 1301-1303; b) W.-Y. Lai, R. Xia, Q.-Y. He, P. A. Levermore, W. Huang, D. D. C. Bradley, *Adv. Mater.* **2009**, *21*, 355-360; c) J. Luo, Y. Zhou, Z.-Q. Niu, Q.-F. Zhou, Y. Ma, J. Pei, *J. Am. Chem. Soc.* **2007**, *129*, 11314-11315.
- [4] a) A. L. Kanibolotsky, R. Berridge, P. J. Skabara, I. F. Perepichka, D. D. C. Bradley, M. Koeberg, *J. Am. Chem. Soc.* **2004**, *126*, 13695-13702; b) W.-Y. Lai, R. Xia, D. D. C. Bradley, W. Huang, *Chem. Eur. J.* **2010**, *16*, 8471-8479; c) Q.-Y. He, W.-Y. Lai, Z. Ma, D.-Y. Chen, W. Huang, *Eur. Polym. J.* **2008**, *44*, 3169-3176; d) W.-Y. Lai, D. Liu, W. Huang, *Macromol. Chem. Phys.* **2011**, *212*, 445-454; e) W. Xu, Z. Kan, T. Ye, L. Zhao, W.-Y. Lai, R. Xia, G. Lanzani, P. Keivanidis, W. Huang, *ACS Appl. Mater. Interfaces* **2015**, *7*, 452-459; f) Y. Jiu, C.-F. Liu, J. Wang, W.-Y. Lai, Y. Jiang, W.-D. Xu, X.-W. Zhang, W. Huang, *Polym. Chem.* **2015**, *6*, 8019-8028; g) C. Cheng, Y. Jiang, C.-F. Liu, J.-D. Zhang, W.-Y. Lai, W. Huang, *Chem. Asian J.* **2016**, *11*, 3589-3597.
- [5] J.-S. Yang, H.-H. Huang, J.-H. Ho, *J. Phys. Chem. B* **2008**, *112*, 8871-8878.
- [6] a) C. Liu, Q. Fu, Y. Zou, C. Zou, D. Ma, J. Qin, *Chem. Mater.* **2014**, *26*, 3074-3083; b) W. Xu, R. Xia, T. Ye, L. Zhao, Z. Kan, Y. Mei, C. Yan, X.-W. Zhang, W.-Y. Lai, P. E. Keivanidis, W. Huang, *Adv. Sci.* **2016**, *3*, 1500245.
- [7] a) F. Liu, W.-Y. Lai, C. Tang, H.-B. Wu, Q.-Q. Chen, B. Peng, W. Wei, W. Wei, Y. Cao, *Macromol. Rapid Commun.* **2008**, *29*, 659-664; b) M. Sang, S. Cao, J. Yi, J. Huang, W.-Y. Lai, W. Huang, *RSC Adv.* **2016**, *6*, 6266-6275; c) J.-P. Yi, L. Zhao, W.-D. Xu, C.-F. Liu, W.-Y. Lai, W. Huang, *J. Mater. Chem. C* **2016**, *4*, 7546-7553; d) M. Fang, J. Huang, Y. Zhang, X. Guo, X. Zhang, C.-F. Liu, W.-Y. Lai, W. Huang, *Mater. Chem. Front.* **2017**, DOI: 10.1039/C6QM00133E.

- [8] a) W.-Y. Lai, R. Zhu, Q.-L. Zhu, L.-T. Hou, Y. Hou, W. Huang, *Macromolecules* **2006**, *39*, 3707-3709; b) W.-Y. Lai, Q.-Q. Chen, Q.-Y. He, Q.-L. Fan, W. Huang, *Chem. Commun.* **2006**, *18*, 1959-1961; c) W.-Y. Lai, Q.-Y. He, R. Zhu, Q.-Q. Chen, W. Huang, *Adv. Funct. Mater.* **2008**, *18*, 265-276; d) P. A. Levermore, R.-D. Xia, W.-Y. Lai, X.-H., Wang, W. Huang, D. D. C. Bradley, *J. Phys. D-Appl. Phys.* **2007**, *40*, 1896-1901; e) W.-Y. Lai, Q.-Y. He, D.-Y. Chen, W. Huang, *Chem. Lett.* **2008**, *37*, 986-987; f) W.-Y. Lai, D. Liu, W. Huang, *Sci. China Chem.* **2010**, *53*, 2472-2480; g) X.-C. Li, C.-Y. Wang, W.-Y. Lai, W. Huang, *J. Mater. Chem. C* **2016**, *4*, 10574-10587; h) X.-C. Li, Y. Zhang, C.-Y. Wang, Y. Wan, W.-Y. Lai, H. Pang, W. Huang, *Chem. Sci.* **2017**, DOI: 10.1039/C6SC05532J.
- [9] a) H. Shang, H. Fan, Y. Liu, W. Hu, Y. Li, X. Zhan, *Adv. Mater.* **2011**, *23*, 1554-1557; b) W.-Y. Lai, X.-R. Zhu, Q.-Y. He, W. Huang, *Chem. Lett.* **2009**, *38*, 392-393; c) C.-F. Liu, Y. Jiu, J. Wang, J. Yi, X.-W. Zhang, W.-Y. Lai, W. Huang, *Macromolecules*, **2016**, *49*, 2549-2558.
- [10] S. Ren, D. Zeng, H. Zhong, Y. Wang, S. Qian, Q. Qian, *J. Phys. Chem. B* **2010**, *114*, 10374-10383.
- [11] D. Katsis, Y. H. Geng, J. J. Ou, S. W. Culligan, A. Culligan, S. H. Chen, L. J. Rothberg, *Chem. Mater.* **2002**, *14*, 1332-1339.
- [12] U. Scherf, K. Müllen, *Makromol. Chem. Rapid Commun.* **1991**, *12*, 489-497.
- [13] a) S. Qiu, P. Lu, X. Lu, F. Z. Shen, L. L. Liu, Y. G. Ma, J. C. Shen, *Macromolecules* **2003**, *36*, 9823-9829; b) J. Jacob, S. Sax, M. Gaal, E. J. W. List, A. C. Grimsdale, K. Müllen, *Macromolecules* **2005**, *38*, 9933-9938; c) Y. Wu, J. Zhang, Z. Zhang, Z. Bo, *J. Am. Chem. Soc.* **2008**, *130*, 7192-7193; d) H. Fan, L. Guo, K. Li, M. S. Wong, K. W. Cheah, *J. Am. Chem. Soc.* **2012**, *134*, 7297-7300; e) L. Guo, K. F. Li, M. S. Wong, K. W. Cheah, *Chem. Commun.* **2013**, *49*, 3597-3599; f) Y. Wu, X. Hao, J. Wu, J. Jin, X. Ba, *Macromolecules* **2010**, *43*, 731-738; g) J. Jacob, S. Sax, T. Piok, E. J. W. List, A. C. List, K. Müllen, *J. Am. Chem. Soc.* **2004**, *126*, 6987-6995; h) G. Zhou, M. Baumgarten, K. Müllen, *J. Am. Chem. Soc.* **2007**, *129*, 12211-12221; i) N. Cocherel, C. Poriol, J. Rault-Berthelot, F. Barriere, N. Audebrand, A. M. Z. Slawin, L. Vignau, *Chem. Eur. J.* **2008**, *14*, 11328-11342; j) K.-T. Wong, L.-C. Chi, S.-C. Huang, Y.-L. Liao, Y.-H. Liu, Y. Wang, *Org. Lett.* **2006**, *8*, 5029-5032; k) H.-H. Huang, C. Prabhakar, K.-C. Tang, P.-T. Chou, G.-J. Huang, J.-S. Yang, *J. Am. Chem. Soc.* **2011**, *133*, 8028-8039; l) G. Zhou, M. Baumgarten, K. Müllen, *J. Am. Chem. Soc.* **2008**, *130*, 12477-12484; m) K. J. Kass, M. Forster, U. Scherf, *Angew. Chem.Int. Ed.* **2016**, *55*, 7816-7820; n) T. Y. Zheng, Z. X. Cai, R. Ho-Wu, S. H. Yau, V. Shaparov, T. Goodson, L. P. Goodson, *J. Am. Chem. Soc.* **2016**, *138*, 868-875; o) L. Guo, K. F. Li, X.-Q. Zhang, K. W. Cheah, M. S. Wong, *Angew. Chem.Int. Ed.* **2016**, *55*, 10639-10644.
- [14] a) H. Kim, N. Schulte, G. Schulte, K. Müllen, F. Laquai, *Adv. Mater.* **2011**, *23*, 894-897; b) R. H. Friend, R. W. Gymer, A. B. Holmes, J. H. Burroughes, R. N. Marks, C. Taliani, D. D. C. Bradley, D. A. D. Santos, J. L. Bredas, M. Logdlund, W. R. Salaneck, *Nature* **1999**, *397*, 121-128; c) J. D. Plumhof, T. Stoferle, L. Mai, U. Scherf, R. F. Mahrt, *Nat. Mater.* **2014**, *13*, 247-252; d) S. Nau, N. Schulte, S. Frisch, J. Frisch, A. Vollmer, N. Koch, S. Sax, E. J. W. List, *Adv. Mater.* **2013**, *25*, 4420-4424.
- [15] B. Kobin, F. Bianchi, S. Halm, J. Leistner, S. Blumstengel, F. Henneberger, S. Hecht, *Adv. Funct. Mater.* **2014**, *24*, 7717-7727.
- [16] J.-S. Yang, H.-H. Huang, Y.-H. Liu, S.-M. Peng, *Org. Lett.* **2009**, *11*, 4942-4945.
- [17] a) W. J. Yang, D. Y. Kim, C. H. Kim, M. Y. Jeong, S. K. Lee, S. J. Jeon, B. R. Cho, *Org. Lett.* **2004**, *6*, 1389-1392; b) Z.-M. Tang, T. Lei, J.-L. Wang, Y. Ma, J. Pei, *J. Org. Chem.* **2010**, *75*, 3644-3655.
- [18] a) W. Xu, J. Yi, W.-Y. Lai, L. Zhao, Q. Zhang, W. Hu, X.-W. Zhang, Y. Jiang, L. Liu, W. Huang, *Adv. Funct. Mater.* **2015**, *25*, 4617-4625; b) J.-L. Wang, Z.-M. Tang, Q. Xiao, Y. Ma, J. Pei, *Org. Lett.* **2009**, *11*, 863-866; c) L. Zhao, C.-F. Liu, W.-D. Xu, Y. Jiang, W.-Y. Lai, W. Huang, *J. Phys. Chem. B* **2015**, *119*, 6730-6739; d) W.-D. Xu, W.-Y. Lai, Q. Hu, X.-Y. Teng, X.-W. Zhang, W. Huang, *Polym. Chem.* **2014**, *5*, 2942-2950.
- [19] Y. Jiang, Y.-X. Lu, Y.-X. Cui, Q.-F. Zhou, Y. Ma, J. Pei, *Org. Lett.* **2007**, *9*, 4539-4542.
- [20] X. H. Zhou, J. C. Yan, J. Pei, *Org. Lett.* **2003**, *5*, 3543-3546.
- [21] Y. Zou, J. Zou, T. Ye, H. Li, C. Yang, H. Wu, D. Ma, J. Qin, Y. Cao, *Adv. Funct. Mater.* **2013**, *23*, 1781-1788.
- [22] Y. Jiang, C. Cheng, J.-J. Cheng, L.-W. Feng, X. Guo, C.-F. Liu, X.-W. Zhang, W.-Y. Lai, W. Huang, *J. Phys. Chem. C* **2015**, *119*, 28117-28126.
- [23] M. F. Zickler, F. A. Feist, J. Jacob, K. Müllen, T. Basche, *Macromol. Rapid Commun.* **2015**, *36*, 1096-1102.
- [24] J. Pommerehne, H. Vestweber, W. Guss, R. F. Guss, H. Bassler, M. Porsch, J. Daub, *Adv. Mater.* **1995**, *7*, 551-554.
- [25] A. G. Crawford, A. D. Dwyer, Z. Liu, A. Steffen, A. Beeby, L.-O. Palsson, D. J. Tozer, T. B. Marder, *J. Am. Chem. Soc.* **2011**, *133*, 13349-13362.
- [26] D. Wasserberg, S. P. Dudek, S. C. J. Meskers, R. A. J. Janssen, *Chem. Phys. Lett.* **2005**, *411*, 273-277.
- [27] R. Xia, G. Heliotis, M. Campoy-Quiles, P. N. Stavrinou, D. D. C. Bradley, D. Vak, D. Y. Vak, *J. Appl. Phys.* **2005**, *98*, 083101.
- [28] a) R. Xia, W.-Y. Lai, P. A. Levermore, W. Huang, D. D. C. Bradley, *Adv. Funct. Mater.* **2009**, *19*, 2844-2850; b) Y. Qian, Q. Wei, G. D. Pozo, M. M. Mroz, L. Lueer, S. Casado, J. Casado, Q. Zhang, L. Xie, R. Xia, W. Huang, *Adv. Mater.* **2014**, *26*, 2937-2942.

## Entry for the Table of Contents

## FULL PAPER

Text for Table of Contents



Yi Jiang,<sup>[a]</sup> Mei Fang,<sup>[a]</sup> Si-Ju Chang,<sup>[a]</sup>  
 Jin-Jin Huang,<sup>[a]</sup> Shuang-Quan Chu,<sup>[a]</sup>  
 Shan-Ming Hu,<sup>[a]</sup> Cheng-Fang Liu,<sup>[a]</sup>  
 Wen-Yong Lai,<sup>\*,[a,b]</sup> Wei Huang<sup>[a,b]</sup>

**Page No. – Page No.**  
**Towards Monodisperse Star-Shaped**  
**Ladder-Type Conjugated Systems:**  
**Design, Synthesis, Stabilized Blue**  
**Electroluminescence and Amplified**  
**Spontaneous Emission**

A novel series of monodisperse star-shaped ladder-type oligo(p-phenylene)s, named as TrL-n (n = 1-3), have been explored with excellent structural perfection free of chemical defects. The resulting materials TrL-n exhibited enhanced spectral stability, suppressed low-energy emission, and superior low ASE thresholds, compared with their corresponding linear ladder-type counterparts FL-m.